

ATOMIC DATA RELEVANT TO LINE FORMATION IN STRONGLY MAGNETIZED WHITE DWARF STARS

G. WUNNER, F. GEYER and H. RUDER

Lehrstuhl für Theoretische Astrophysik der Universität
Tübingen, Tübingen, F.R.G.

ABSTRACT. The discovery of magnetic field strengths in the range of 500 million Gauss in the objects Grw+70°8247 and PG1031+224 has given enormous impetus to investigations of magnetic white dwarf stars. We have determined intensities of Balmer transitions for $B > 10^6$ Gauss as a function of field and find strong oscillations of the transitions strengths, which are of importance to the quantitative analysis of the observed spectra and the interpretation of polarimetric measurements in these objects.

The spectroscopic detection of very strong magnetic fields in white dwarf stars, and the measurement of their absolute sizes, was hampered, in the past, by the fact that the linear and quadratic Zeeman effect as well as other perturbational methods (Kemic 1974) fail once the magnetic field strength exceeds ~ 10 MGauss. It was only recently that the results of exact quantum mechanical calculations became available for the energy levels of moderately excited states of the hydrogen atom, and the strengths of electromagnetic transitions between them, at magnetic field strengths that extend way up to those encountered in neutron stars ($\sim 5 \times 10^{12}$ Gauss) (Forster et al. 1984, Ruder et al. 1986). On the basis of these calculations it has now become possible to unambiguously account for the wavelength positions of hitherto unexplained spectral features in Grw+70°8247 in terms of "stationary" components of Balmer and Paschen transitions in a magnetic field of ~ 350 MGauss (Angel et al. 1985, Greenstein et al. 1985, Wunner et al. 1985). Additional support for this argument has come from the identification of similar features in the UV and optical spectra of PG1031+234 by Schmidt et al. (1986), who find evidence for a magnetic field strength of up to 500 MGauss. No systematic analysis, however, has been performed so far as to the intensities and line shapes of the observed features. It is the purpose of this note to point out that the strengths of relevant stationary transitions go through strong oscillations over the range of field which is of interest in these objects. The discovery of these oscillations adds an additional complication - and a challenge - to actual calculations of theoretical line shapes and intensities, which certainly are urgent.

Paper presented at the IAU Colloquium No. 93 on 'Cataclysmic Variables. Recent Multi-Frequency Observations and Theoretical Developments', held at Dr. Remeis-Sternwarte Bamberg, F.R.G., 16–19 June, 1986.

Astrophysics and Space Science 131 (1987) 595–599.
© 1987 by D. Reidel Publishing Company.

The main problem in determining the energies and wave functions of hydrogen atoms in magnetic fields of arbitrary strength lies in the fact that the contradicting symmetries - spherical symmetry for the Coulomb field of the nucleus, cylindrical symmetry for the external magnetic field - do not allow a separation of variables. A hydrogen atom in a magnetic field thus represents one of the simplest examples of a "non-integrable" system. One therefore has to resort to some numerical method or another. We expanded the wave functions in terms of spherical harmonics, and the radial expansion functions in a complete, orthonormal basis set of Laguerre functions with fixed exponent. In this basis, the Hamiltonian matrix assumes a banded form, and can be diagonalized by use of efficient standard algorithms. The maximum basis dimension used in the present work is 3600. The computations were performed on the Cray-1 machine of the University of Stuttgart.

Accuracies of at least 6 significant figures are obtained for energy values, and of at least 3 significant figures for transition strengths. Results for the behaviour of the energy levels of the states evolving from the field-free states with negative parity and principal quantum numbers $n=4, 5$ are shown in Fig. 1a (magnetic quantum number $m=0$) and Fig. 2a ($m=-1$). The magnetic field parameter β used in the figures is given by $\beta = B/B_0$, with $B_0 = 2(\alpha mc)^2/(e\hbar) \approx 4700$ MGauss. Noteworthy is the wavy shape of the curves drawn. This is in fact a behaviour typical of energy levels of non-integrable systems in general: two adjacent levels which first approach each other as a function of an external parameter (here the magnetic field) finally repel - in accordance with the Wigner-von Neumann non-crossing rule of quantum mechanics - and thus go through an "avoided" crossing, in which the characters of the wave functions are interchanged. These avoided crossings become more and more pronounced the higher one goes with the principal quantum number, and for $n > 30$ are even observable at laboratory field strengths. The exchange of the types of the wave functions in every avoided crossing is the reason for the strong sensitivity of the dipole matrix elements with respect to variations of the magnetic field, shown in Fig. 1b and Fig. 2b for the stationary H_β and H_γ transitions from $2s$ to the states of Fig. 1a and Fig. 2a, respectively. Zeroes and extrema of the matrix elements are obviously correlated with avoided crossings of the levels involved in the transitions. It is evident that the strong oscillations found for the transition strengths can decisively influence the observability and line shapes of stationary components. Numbers for wavelengths and dipole strengths (square of the dipole matrix element), which can be used in calculations of synthetic spectra, are presented in Table 1 and Table 2. The grid for the field strength in the tables is much finer than in previous calculations, which therefore failed to accurately describe the strong oscillations of the transition strengths.

Similar oscillations occur also for non-stationary components, and there arises the possibility for non-stationary components to produce observable effects if the transition strength is sharply peaked around a maximum in the neighbourhood of an avoided crossing of the final state. Quantitative calculations in this direction are in progress.

This work was supported by the Deutsche Forschungsgemeinschaft.

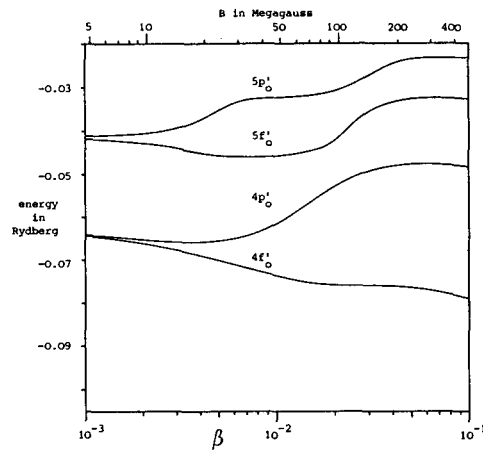


Fig. 1a. Energy levels of the hydrogen atom belonging to principal quantum numbers $n = 4$ and 5 , negative parity, and magnetic quantum number $m = 0$ in the range of magnetic field strength 4.7 to 470 Megagauss. Note the occurrence of "avoided" level crossings.

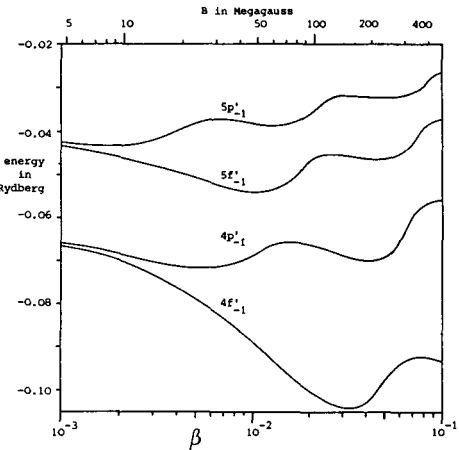


Fig. 2a. Energy levels of the hydrogen atom belonging to principal quantum numbers $n = 4$ and 5 , negative parity, and magnetic quantum number $m = -1$ in the range of magnetic field strength 4.7 to 470 Megagauss. Here the avoided crossings are even more pronounced.

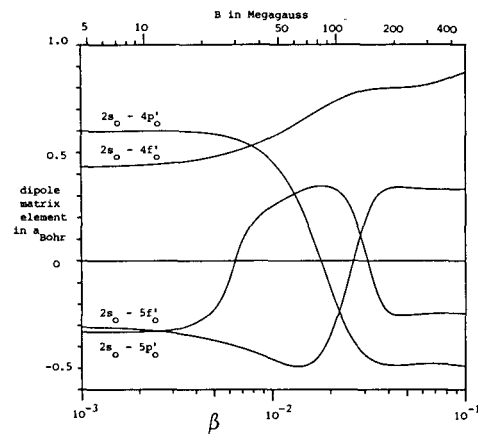


Fig. 1b. Dipole matrix elements of stationary Balmer transitions (n components) from $2s$ to the states shown in the energy diagram above as a function of field strength. Evidently the avoided level crossings, where states exchange the characters of their wave functions, can cause strong oscillations of the dipole transition strengths in a range of field where the wavelengths of the transitions become stationary. Obviously this can lead to selection effects in the observability of stationary components at values of the magnetic field strength where a dipole matrix element goes through zero.

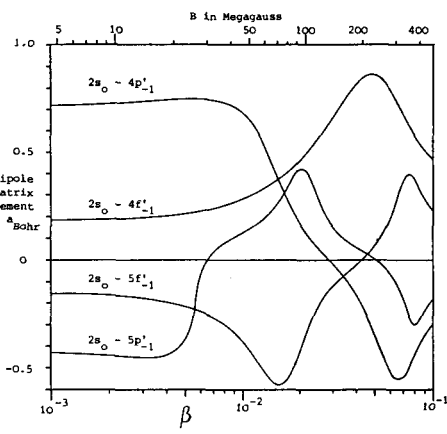


Fig. 2b. Dipole matrix elements of stationary Balmer transitions (n components) from $2s$ to the states shown in the energy diagram above as a function of field strength. Again the avoided crossings are reflected in a strong B -dependence of the transition strengths.

Table 1. Wavelengths and dipole strengths (as defined by Forster et al. 1984) of stationary Balmer transitions (π components) as a function of the magnetic field parameter β . Upper entry: wavelength in Å; lower entry: dipole strength in atomic units.

	β												
Trans.	1.00(-3)	1.50(-3)	2.00(-3)	3.00(-3)	5.00(-3)	5.50(-3)	6.00(-3)	6.50(-3)	7.00(-3)	7.50(-3)	8.00(-3)	8.50(-3)	1.00(-2)
2s - 4f'0	4860.70 1.90(-1)	4858.19 1.92(-1)	4854.72 1.96(-1)	4845.10 2.05(-1)	4816.74 2.33(-1)	4808.09 2.41(-1)	4798.94 2.49(-1)	4789.34 2.58(-1)	4779.33 2.68(-1)	4768.96 2.77(-1)	4758.28 2.87(-1)	4747.33 2.97(-1)	4713.23 3.29(-1)
2s - 4p'0	4855.52 3.61(-1)	4846.69 3.61(-1)	4834.66 3.61(-1)	4802.21 3.60(-1)	4712.75 3.44(-1)	4687.03 3.37(-1)	4660.48 3.28(-1)	4633.32 3.18(-1)	4605.74 3.06(-1)	4577.91 2.93(-1)	4549.99 2.79(-1)	4522.11 2.63(-1)	4439.76 2.10(-1)
2s - 5f'0	4336.78 9.44(-2)	4330.92 9.78(-2)	4323.24 1.02(-1)	4303.80 1.12(-1)	4255.75 1.37(-1)	4242.75 1.44(-1)	4229.52 1.51(-1)	4216.12 1.58(-1)	4202.59 1.65(-1)	4188.95 1.73(-1)	4175.23 1.80(-1)	4161.63 1.88(-1)	4119.73 2.10(-1)
2s - 5p'0	4324.77 1.09(-1)	4304.96 1.10(-1)	4279.35 1.09(-1)	4216.22 1.02(-1)	4073.01 5.12(-2)	4039.49 2.80(-2)	4009.76 6.77(-3)	3985.32 1.86(-4)	3965.69 8.26(-3)	3949.05 2.04(-2)	3934.07 3.17(-2)	3920.03 4.12(-2)	3880.95 6.33(-2)

	β												
Trans.	1.25(-2)	1.30(-2)	1.35(-2)	1.40(-2)	1.45(-2)	1.50(-2)	1.60(-2)	1.70(-2)	1.80(-2)	1.90(-2)	2.00(-2)	2.20(-2)	2.40(-2)
2s - 4f'0	4654.04 3.82(-1)	4642.09 3.93(-1)	4630.15 4.04(-1)	4618.23 4.14(-1)	4606.36 4.25(-1)	4594.55 4.35(-1)	4571.17 4.55(-1)	4548.20 4.74(-1)	4525.71 4.93(-1)	4503.78 5.10(-1)	4482.47 5.26(-1)	4441.88 5.54(-1)	4404.19 5.76(-1)
2s - 4p'0	4311.58 1.15(-1)	4287.78 9.65(-2)	4264.66 7.92(-2)	4242.25 6.31(-2)	4220.55 4.85(-2)	4199.58 3.55(-2)	4159.79 1.53(-2)	4122.82 3.39(-3)	4088.56 0.34(-4)	4056.83 4.50(-3)	4027.47 1.55(-2)	3975.01 5.04(-2)	3929.72 9.21(-2)
2s - 5f'0	4049.53 2.38(-1)	4035.41 2.41(-1)	4021.28 2.43(-1)	4007.13 2.42(-1)	3992.98 2.39(-1)	3978.84 2.27(-1)	3950.58 2.08(-1)	3922.44 1.84(-1)	3894.54 1.54(-1)	3866.98 1.23(-1)	3839.90 6.24(-2)	3787.60 1.86(-2)	3738.55
2s - 5p'0	3821.21 9.01(-2)	3809.85 9.46(-2)	3798.66 9.88(-2)	3787.64 1.03(-1)	3776.79 1.06(-1)	3766.10 1.09(-1)	3745.20 1.15(-1)	3724.92 1.18(-1)	3705.25 1.19(-1)	3686.16 1.18(-1)	3667.64 1.15(-1)	3632.12 1.01(-1)	3598.32 7.84(-2)

	β												
Trans.	2.60(-2)	2.80(-2)	3.00(-2)	3.20(-2)	3.40(-2)	3.60(-2)	3.80(-2)	4.00(-2)	5.00(-2)	6.30(-2)	7.00(-2)	8.00(-2)	1.00(-1)
2s - 4f'0	4369.51 5.94(-1)	4337.84 6.08(-1)	4309.13 6.18(-1)	4283.26 6.25(-1)	4260.05 6.30(-1)	4239.35 6.33(-1)	4220.98 6.35(-1)	4204.75 6.36(-1)	4150.06 6.41(-1)	4124.85 6.59(-1)	4124.56 6.75(-1)	4133.68 7.02(-1)	4167.42 7.61(-1)
2s - 4p'0	3890.42 1.32(-1)	3856.15 1.64(-1)	3826.20 1.89(-1)	3799.97 2.07(-1)	3776.96 2.19(-1)	3756.77 2.27(-1)	3739.04 2.31(-1)	3723.49 2.33(-1)	3670.57 2.32(-1)	3641.86 2.28(-1)	3637.51 2.28(-1)	3639.18 2.31(-1)	3655.43 2.40(-1)
2s - 5f'0	3693.53 4.50(-4)	3653.26 7.26(-3)	3618.20 3.01(-2)	3588.34 5.71(-2)	3563.19 7.97(-2)	3542.02 9.55(-2)	3524.07 1.05(-1)	3508.74 1.11(-1)	3458.33 1.13(-1)	3430.66 1.09(-1)	3425.71 1.08(-1)	3425.61 1.07(-1)	3437.03 1.09(-1)
2s - 5p'0	3565.77 4.97(-2)	3534.12 2.14(-2)	3503.46 2.97(-3)	3474.58 1.67(-3)	3448.64 1.53(-2)	3426.43 3.36(-2)	3407.92 4.82(-2)	3392.51 5.73(-2)	3344.05 6.48(-2)	3317.76 6.12(-2)	3312.80 6.01(-2)	3312.15 5.95(-2)	3321.42 6.03(-2)

Table 2. Wavelengths and dipole strengths (as defined by Forster et al. 1984) of stationary Balmer transitions (σ components) as a function of the magnetic field parameter β . Upper entry: wavelength in Å; lower entry: dipole strength in atomic units.

β													
Trans.	1.00(-3)	1.50(-3)	2.00(-3)	2.50(-3)	3.00(-3)	4.00(-3)	5.00(-3)	6.00(-3)	7.00(-3)	8.00(-3)	9.00(-3)	1.00(-2)	1.10(-2)
2s -	4911.37	4933.24	4953.49	4972.16	4989.32	5019.37	5044.27	5064.64	5081.05	5094.01	5103.97	5111.30	5116.31
4f'-1	3.39(-2)	3.46(-2)	3.55(-2)	3.67(-2)	3.82(-2)	4.16(-2)	4.59(-2)	5.10(-2)	5.69(-2)	6.35(-2)	7.09(-2)	7.92(-2)	8.83(-2)
2s -	4902.80	4914.06	4919.75	4920.27	4916.04	4895.27	4861.18	4817.25	4766.52	4711.62	4654.92	4598.58	4544.61
4p'-1	5.19(-1)	5.24(-1)	5.30(-1)	5.37(-1)	5.43(-1)	5.55(-1)	5.62(-1)	5.61(-1)	5.53(-1)	5.35(-1)	5.07(-1)	4.66(-1)	4.12(-1)
2s -	4373.54	4382.77	4388.29	4390.72	4390.67	4385.03	4374.34	4360.33	4343.87	4325.27	4304.45	4281.02	4254.39
5f'-1	2.38(-2)	2.53(-2)	2.73(-2)	2.97(-2)	3.25(-2)	3.92(-2)	4.75(-2)	5.81(-2)	7.17(-2)	8.96(-2)	1.13(-1)	1.44(-1)	1.83(-1)
2s -	4357.85	4348.66	4330.26	4304.52	4273.16	4199.63	4122.53	4073.22	4045.66	4021.07	3997.84	3975.61	3954.11
5p'-1	1.84(-1)	1.90(-1)	1.97(-1)	2.02(-1)	2.04(-1)	1.96(-1)	1.34(-1)	4.41(-3)	1.40(-3)	6.00(-3)	1.07(-2)	1.56(-2)	2.12(-2)
β													
Trans.	1.20(-2)	1.30(-2)	1.40(-2)	1.50(-2)	1.60(-2)	1.70(-2)	1.80(-2)	1.90(-2)	2.00(-2)	2.20(-2)	2.40(-2)	2.60(-2)	2.80(-2)
2s -	5119.27	5120.40	5119.89	5117.88	5114.52	5109.90	5104.12	5097.25	5089.36	5070.73	5048.60	5023.26	4995.00
4f'-1	9.83(-2)	1.09(-1)	1.21(-1)	1.34(-1)	1.48(-1)	1.63(-1)	1.79(-1)	1.96(-1)	2.14(-1)	2.54(-1)	2.97(-1)	3.44(-1)	3.93(-1)
2s -	4494.84	4450.63	4412.59	4380.47	4353.38	4330.29	4310.25	4292.52	4276.58	4248.64	4224.46	4202.99	4183.57
4p'-1	3.48(-1)	2.78(-1)	2.12(-1)	1.55(-1)	1.11(-1)	7.84(-2)	5.54(-2)	3.91(-2)	2.74(-2)	1.30(-2)	5.39(-3)	1.53(-3)	0.75(-4)
2s -	4223.91	4189.19	4150.53	4109.06	4066.51	4024.83	3985.79	3950.69	3920.15	3871.80	3835.91	3807.68	3784.31
5f'-1	2.28(-1)	2.74(-1)	3.11(-1)	3.31(-1)	3.32(-1)	3.12(-1)	2.76(-1)	2.30(-1)	1.83(-1)	1.05(-1)	6.03(-2)	3.60(-2)	2.23(-2)
2s -	3933.09	3912.29	3891.41	3870.10	3847.94	3824.48	3799.32	3772.40	3744.26	3689.21	3643.79	3609.85	3583.78
5p'-1	2.81(-2)	3.69(-2)	4.84(-2)	6.35(-2)	8.33(-2)	1.08(-1)	1.35(-1)	1.61(-1)	1.77(-1)	1.61(-1)	1.06(-1)	6.08(-2)	3.56(-2)
β													
Trans.	3.00(-2)	3.20(-2)	3.40(-2)	3.60(-2)	3.80(-2)	4.00(-2)	5.00(-2)	6.00(-2)	6.30(-2)	7.00(-2)	8.00(-2)	9.00(-2)	1.00(-1)
2s -	4964.12	4930.95	4895.85	4859.29	4821.58	4783.35	4602.04	4477.04	4450.08	4422.44	4413.53	4427.19	4450.85
4f'-1	4.43(-1)	4.94(-1)	5.43(-1)	5.89(-1)	6.32(-1)	6.69(-1)	7.41(-1)	6.21(-1)	5.67(-1)	4.51(-1)	3.34(-1)	2.64(-1)	2.19(-1)
2s -	4165.76	4149.21	4133.62	4118.73	4104.28	4090.01	4012.74	3913.25	3881.70	3818.98	3772.97	3762.45	3766.16
4p'-1	3.95(-4)	2.27(-3)	5.71(-3)	1.09(-2)	1.80(-2)	2.74(-2)	1.22(-1)	2.69(-1)	2.97(-1)	2.91(-1)	1.92(-1)	1.24(-1)	8.92(-2)
2s -	3764.32	3746.88	3731.48	3717.78	3705.51	3694.47	3651.81	3615.43	3602.33	3564.34	3513.11	3494.87	3494.22
5f'-1	1.41(-2)	8.96(-3)	5.50(-3)	3.14(-3)	1.54(-3)	5.39(-4)	4.05(-3)	3.81(-2)	6.10(-2)	1.21(-1)	1.39(-1)	7.95(-2)	4.99(-2)
2s -	3562.57	3544.59	3528.99	3515.29	3503.17	3492.41	3453.79	3430.63	3424.76	3409.04	3376.39	3357.15	3355.34
5p'-1	2.21(-2)	1.45(-2)	9.84(-3)	6.78(-3)	4.66(-3)	3.14(-3)	0.10(-4)	4.19(-3)	8.81(-3)	3.47(-2)	8.98(-2)	5.72(-2)	3.25(-2)

REFERENCES

- Angel, J. R. P., et al., *Astrophys. J.*, **292**, 260 (1985)
 Forster, H. G., et al., *J. Phys. B*, **17**, 1301 (1984)
 Greenstein, J. L., et al., *Astrophys. J.*, **289**, L25 (1985)
 Kemic, S. B., *Joint Inst. Lab. Astrophys. Rep.* No. 113 (1974)
 Ruder, H., et al., *Physics Reports*, in preparation (1986)
 Schmidt, G. D., et al., *Astrophys. J.*, in press (1986)
 Wunner, G., et al., *Astron. Astrophys.*, **149**, 102 (1985)